HHS Public Access

Author manuscript

J Bone Miner Res. Author manuscript; available in PMC 2017 February 01.

Published in final edited form as:

J Bone Miner Res. 2016 February ; 31(2): 416–429. doi:10.1002/jbmr.2698.

Deletion of the distal *Tnfsf11* RL-D2 enhancer that contributes to PTH-mediated RANKL expression in osteoblast lineage cells results in a high bone mass phenotype in mice

M. Onal, **H.C. St John**, **A.L. Danielson**[1], and **J.W. Pike**[2,3]

Department of Biochemistry, University of Wisconsin-Madison, Madison, WI. 53706 USA

Abstract

Receptor activator of nuclear factor-κB ligand (RANKL) is a TNF-like cytokine that is necessary for osteoclast formation and survival. Elevated RANKL synthesis is associated with both increased osteoclast number and bone resorption. Earlier studies identified an enhancer 76 kb upstream of the *Tnfsf11* transcriptional start site (TSS) termed RL-D5 or the distal control region (DCR) that modulates RANKL expression in response to PTH, $1,25(OH)_2D_3$, and an array of cytokines. Mice lacking RL-D5 exhibit high bone mass associated with decreased RANKL expression in bone, spleen, and thymus. In addition to RL-D5, genome-wide studies have identified 9 additional *Tnfsf11* enhancers residing upstream of the gene's TSS, which provide RANKL cell type-specificity and responsiveness to local and systemic factors. ChIP-chip analysis has revealed inducible VDR and CREB binding at an enhancer termed RL-D2 23 kb upstream of the *Tnfsf11* TSS in osteoblastic ST2 cells. Herein, we use ChIP-seq analysis to confirm this finding and delete this enhancer from the mouse genome to determine its physiological role in vivo. RL-D2$^{-/-}$ primary stromal cells showed decreased RANKL-induction by both forskolin and $1,25(OH)_2D_3$ ex vivo. Consistent with this, the PTH induction of RANKL expression was significantly blunted in RL-D2$^{-/-}$ mice in vivo. In contrast, lack of RL-D2 had no effect on $1,25(OH)_2D_3$ induction of RANKL in vivo. Similar to the results seen in RL-D5$^{-/-}$ mice, lack of RL-D2 led to decreased skeletal RANKL expression, resulting in decreased osteoclast numbers and a progressive increase in bone mineral density. Lack of RL-D2 increased cancellous bone mass in femur and spine, but did not alter femoral cortical bone thickness. These results highlight the role of distal enhancers in the regulation of RANKL expression by PTH and perhaps $1,25(OH)_2D_3$, and suggest that the RL-D2 and RL-D5 enhancers contribute in either an additive or synergistic manner to regulate bone remodeling.

[3]Please send correspondence to: Professor J. Wesley Pike, Department of Biochemistry, University of Wisconsin-Madison, Hector F. Deluca Laboratories, Room 543D, 433 Babcock Drive, Madison, WI 53706; Phone (608) 262-8229; Fax (608) 263-9609; pike@biochem.wisc.edu.

1Current address: Northwestern Health Sciences University, Bloomington, MN 55431 USA

2This work was supported by NIH NIAMS grant AR-074993 to JWP

Supplemental information is included with the manuscript

Disclosure: The authors declare no conflict of interest

Authors' roles: Study design: JWP and MO. Study conduct: MO. Data collection: MO, ALD and HCS. Data analysis: MO. Data interpretation: MO and JWP. Drafting manuscript: JWP and MO. Revising manuscript content: MO and JWP. Approving final version of manuscript: JWP. JWP takes responsibility for the integrity of the data analysis.

Keywords

RANKL; PTH; $1,25D_3$; transcriptional regulation

INTRODUCTION

Receptor activator of nuclear factor-κB ligand (RANKL) is a multifunctional cytokine that participates in a variety of physiological processes such as organ development [1–3], control of fever and body temperature [4], lymphocyte differentiation [1,5], and mammary gland development [6]. One of the most significant roles of RANKL is to regulate bone remodeling and calcium homeostasis by controlling osteoclast formation and survival [1,7,8]. Mice that lack RANKL, or its receptor RANK, cannot form osteoclasts and thus, have osteopetrosis and a blockade in tooth eruption, illustrating the necessity of RANKL for osteoclast formation [1]. In addition to defects emerging from the lack of osteoclast formation, animals that lack RANKL also fail to develop mammary glands and lymph nodes [1,8].

As expected from its diverse roles, RANKL is expressed in a wide array of cell types that contribute to differential functions of RANKL. RANKL expression in chondrocytes is important for resorption of the calcified cartilage to produce the bone marrow cavity in long bones of growing mice [9] whereas, osteocytic RANKL is the major functional source of RANKL for physiological bone remodeling in adult mice [9,10]. Moreover, while B or T cell RANKL does not appear to participate in physiological bone remodeling in adult mice, B cell RANKL plays a role in B cell differentiation and in the cancellous bone loss associated with loss of sex steroids [5]. An increase in RANKL leads to increased osteoclast formation and survival, thus leading to increased bone resorption. Consistent with this, increased RANKL has been associated with a number of pathological conditions such as hyperparathyroidism [11,12] and arthritis [13,14]. Thus, the mechanisms that mediate transcriptional control of RANKL leading to cell type-specific expression and regulation are of great biological importance in many physiological and pathophysiological conditions.

Initial transcriptional studies examining the $1,25(OH)_2D_3$ and parathyroid hormone (PTH) regulation of *Tnfsf11* expression focused on *Tnsfs11*'s modulatory control by elements located near the promoter region of the gene [15,16]. These earlier studies were either inconclusive or unsuccessful, largely as a result of the limitations of the approach. Our application of recently developed genome-wide methods for defining the transcriptional landscape of genes [17,18]; however, has revealed that *Tnfsf11* is regulated by at least 10 different distal enhancers [19–25]. These enhancers extend up to 155 kb upstream of the gene's transcriptional start site (TSS) and are bound by various transcription factors associated with pathways that control RANKL expression as summarized in Fig. 1. The number, distal nature, and diverse activities of these enhancers are consistent with the regulatory features of many genes whose products are involved in diverse transcriptional control. Perhaps as important, we have recently shown that a DNA segment beginning 46 kb downstream to 178 kb upstream of the *Tnfsf11* gene and containing all of these elements is capable of expressing RANKL in an endogenous tissue-specific and regulated fashion, and rescues the phenotype of the RANKL null mice in a comprehensive fashion [26]. Although

this latter study does not define the individual roles of the internal features of the *Tnfsf11* gene, the studies collectively highlight the unexpected complexity of RANKL regulation.

Six of the RANKL enhancers, termed RL-D1 to RL-D4 and RL-D6 and RL-D7 were identified in osteoblast cell lines [19,22,24,27] and are suggested to regulate RANKL expression in mesenchymal lineage cells. In contrast, three of the RANKL enhancers, termed RL-T1 to RL-T3, were identified in T cell lines [23,28] and suggested to play roles in transcriptional regulation of RANKL in certain hematopoietic lineage cells. The RL-D5 enhancer, however, is bound by transcription factors in both osteoblasts and T cell lines [21,23,28,29]. This enhancer has been identified by us and others as a multifunctional component that regulates transcriptional control of RANKL in response to PTH, $1,25(OH)_2D_3$, and interleukin 6 (IL-6)-type cytokines both in vitro and in vivo [19,21,29,30]. Importantly, lack of this enhancer in the mouse genome decreased RANKL expression in bone, spleen, and thymus and led to an age-dependent high bone mass phenotype [12,30]. RL-D5 was also shown to play a role in secondary hyperparathyroidism- and lactation-induced increase in RANKL expression [12]. However, the physiological and tissue-specific roles of the remaining RANKL enhancers have yet to be defined.

RL-D2 is a RANKL enhancer located 23 kb upstream of the *Tnsfsf11* TSS [19]. Chromatin immunoprecipitation on microarray (ChIP-chip) analysis in osteoblastic ST2 cells has shown inducible binding of vitamin D receptor (VDR), retinoid X receptor (RXR), runt-related transcription factor 2 (Runx2), and cAMP response element-binding protein (CREB) within this enhancer [19,21]. In addition, ChIP-chip analysis has shown that parts of the transcriptional machinery such as TATA-binding protein (TBP), Transcription Factor II B (TFIIB), transcription initiation factor TFIID 250 kDa subunit (TAF250), and RNA polymerase II (RNA pol II) are recruited to this enhancer in an inducible manner [22,27]. This DNA segment was also marked by the enhancer histone signature modifications H4ac and H3K9ac in osteoblastic ST2 cells [22], but not in 2b4.11 T cell hybridomas or in primary $CD4^+$ T cells [23]. Together, these results suggest that RL-D2 plays a role in transcriptional control of RANKL specifically in cells of mesenchymal origin, although in vivo studies are necessary to validate this hypothesis. Herein, we confirm the binding of VDR, RXR, and CREB to this enhancer in a pre-osteoblastic cell line (MC3T3-E1). We then delete this enhancer from the mouse genome to assess its contribution to both cell type-specific and hormonal regulation of RANKL expression and to examine its role during physiologic perturbation in vivo. We show that while both PTH- and $1,25(OH)_2D_3$- induction of RANKL expression are blunted as a result of the lack of RL-D2 ex vivo, only the PTH induction of RANKL expression was blunted in vivo. In addition, mice that lack RL-D2 exhibited lower RANKL expression in bone, bone marrow, and spleen, but not in thymus or isolated lymphocytes. This decrease in skeletal RANKL caused RL-D2 null mice to display decreased bone resorption and a resultant high bone mass phenotype that progressed with age.

MATERIALS AND METHODS

Reagents

Minimum Eagle's medium alpha (αMEM) and Hank's balanced salt solution were purchased from MediaTech/cellgro (Manassas, VA); Fetal bovine serum (FBS), and penicillin-streptomycin-L-glutamine (PSG) were purchased from Hyclone (Logan, UT); and ascorbic acid was purchased from Sigma Aldrich (St. Louis, MO). Cultured MC3T3-E1 cells were treated with $1,25(OH)_2D_3$ obtained from SAFC Global (Madison, WI), forskolin (Fsk) purchased from Sigma Aldrich (St. Louis, MO) or oncostatin M (OSM) purchased from R&D Systems (Minneapolis, MN). PTH (1–84) used for the in vivo injections were purchased from Bachem California Inc. (Torrance, CA). The VDR (C-20, sc-1008, lot A0912) and RXR (N-197, sc-774, lot G2310) antibodies used for chromatin immunoprecipitation (ChIP) were purchased from Santa Cruz Biotechnology, Inc. (Santa Cruz, CA). The phosphorylated CREB (pCREB) (Ser 133, 06-519) antibody used for ChIP was purchased from Millipore (Darmstadt, Germany).

Generation of mutant mice

D2KO mice were produced by GenOway (Strasbourg, Fr). Briefly, D2KO mice were created by replacing the 2.1 kb RL-D2 enhancer with a targeting vector consistent of a floxed *Neo* selection cassette flanked by 7.2 kb left homology arm and 2.5 kb right homology arm. The 7.2 kb left homology arm was produced by PCR amplification of 3 kb proximal and 4.2 kb distal regions using genomic C57BL/6 ES cell DNA and *Tnfsf11* BAC as templates, respectively. The right homology arm was PCR amplified using genomic C57BL/6 ES cell DNA as template. The resultant PCR products were cloned into a vector to produce the targeting vector containing the *Neo* selection cassette flanked by the left and right homology arms. Sequencing was utilized at every step of the targeting vector assembly to control the quality. The linearized targeting vector was used to electroporate ES cells. The ES cells targeted by homologous recombination were identified by positive selection using G418 treatment, followed by confirmation via PCR and southern blot analysis of the homology arms. Two correctly targeted ES cell clones were injected into C57BL/6 blastocyts to create chimeric mice. Injected blastocyts were then re-implanted into OF1 pseudo-pregnant females and allowed to develop. The neo cassette was removed by crossing the germ line transmitting chimeric mice with mice ubiquitously expressing Cre recombinase. The animals were genotyped using the forward primer 5′-TCAGAAGTTGCGCACGGTCAGC-3′ and reverse primer 5′-ACAGATCTGCGGCCGCTCTAGTA-3′. Mice heterozygous for the RL-D2 enhancer ($D2^{+/-}$) were used as breeders to obtain the experimental animals RL-$D2^{+/+}$ (D2WT) and RL-$D2^{-/-}$ (D2KO) mice. In all experiments, RL-D2 wild type (D2WT) littermates were used as controls for RL-D2 knock out (D2KO) mice.

Animal Studies

The animals were housed in high density ventilated caging in the Animal Research Facility of University of Wisconsin-Madison. The husbandry rooms were monitored for 12 hour light/dark cycles, 72°F temperature and 45% humidity. To induce RANKL expression in vivo, animals were injected intraperitoneally with 10 ng/g of body weight (bw) $1,25(OH)_2D_3$ (in propylene glycol) or 230 ng/g bw PTH (1–84) (in phosphate buffered saline). The

animals were stratified to vehicle or treatment groups according to their body weight. The littermate controls were injected with a similar volume of appropriate vehicle. Animals were sacrificed and tissues collected 6 hours (hrs) after $1,25(OH)_2D_3$ or 1 hour (hr) after PTH injection. All injections and tissue collections were performed in the procedure rooms in the Research Animal Facility of University of Wisconsin-Madison. All animal studies were reviewed and approved by the Research Animal Care and Use Committee of University of Wisconsin-Madison.

Primary Stromal Cell Cultures

Femoral bone marrow was isolated using Hank's isolation medium (MEMα with Hank's Salts supplemented with 10% non-heat inactivated FBS and 1% PSG). The isolated cells were plated into 12 well plates with a density of $5x10^6$ cells/well in 1 ml osteogenic culture media (MEMα without phenol red, supplemented with 10% non-heat inactivated FBS, 1% PSG and 50 ug/ml ascorbic acid). Cells were differentiated and cultured to 90% confluency (8 to 10 days) by changing the top half of the culture media every 2 days. At ~90% confluency, cells were washed with phosphate buffered saline (PBS), all of the media was replaced with fresh culture media containing vehicle or treatments. In order to induce RANKL expression, differentiated osteoblastic stromal cell cultures were treated with 25 ng/ml of OSM in PBS, 10^{-8} M $1,25(OH)_2D_3$ in ethanol, or 10^{-6} M for forskolin in dimethyl sulfoxide (DMSO) for 24 hrs. Following 24 hrs treatment, RNA was isolated from cultured cells using Trizol Reagent (Life technologies, Grand Island, NY) according to the manufacturer's instructions.

Primary stromal cell cultures for chromatin immunoprecipitation (ChIP) were prepared as follows. Femoral and humoral bone marrow cells were isolated using osteogenic culture media (MEMα without phenol red, supplemented with 10% non-heat inactivated FBS, 1% PSG and 50 μg/ml ascorbic acid) and plated at a density of $1x10^8$ cells/well in 10 ml of culture media. Cells cultured to 90% confluency (9 days) in osteogenic medium by changing the top half of the culture media every 2 days for the first week, followed by daily complete media change beginning at day 7. At day 9, cells were washed with phosphate buffered saline (PBS) and fresh culture media containing DMSO or 10^{-6} M forskolin (Fsk) was added.

Chromatin immunoprecipitation (ChIP)

ChIP-qPCR analysis was performed in triplicate as previously described [(22)]. Following hormonal treatment as described above, the primary cell cultures were cross-linked for 15 min with 1.5% formaldehyde in PBS and the reaction was quenched using 1.25 M glycine. Cell extracts were collected in PBS and chromatin fragments prepared via sonication. Samples were then pre-cleared over night, followed by immunoprecipitation using either a control IgG or pCREB (ser 133) antibody. After washing, the protein-DNA crosslinks were reversed and the DNA fragments were purified using a QIAquick PCR kit (Qiagen, Valencia, CA). Quantitative RT-PCR was performed using Fast Start Universal Sybr green (Roche Applied Science, Indianapolis, IN) and primers designed to amplify the control region 30kb upstream of *Mmp13* TSS, as well as the RL-D2, RL-D4 and RL-D5 enhancer regions of the *Tnfsf11* locus.

ChIP followed by sequencing (ChIP-seq)

ChIP-seq data processing and statistical evaluation were performed as previously described [31]. Briefly, pre-osteoblastic MC3T3-E1 cells were treated for 1 hr with vehicle or 10^{-6} M Fsk; or for 3 hrs with vehicle or 10^{-7} M $1,25(OH)_2D_3$ (32,33). After fixation, samples were subjected to immunoprecipitation using either a control IgG antibody or experimental antibody (pCREB (ser 133), VDR and RXR antibodies listed under "Reagents" section). All sequencing data are publically available in the Gene Expression Omnibus database: GSE62981 and GSE51515 [32,33].

Bone Mineral Density (BMD) and μCT Analysis

BMDs were measured and analyzed by dual x-ray absorptiometry (DEXA) with a PIXImus densitometer (GE-Lunar Corp, Madison, WI) as previously described [34]. Lumbar vertebrae 4 (L4) and femurs were fixed in 10% Millonig's Modified Buffered Formalin (Leica Biosystems, Richmond, IL) for 24 hrs and gradually dehydrated through a series of ethanol solutions into 100% ethanol. MicroCt analysis of the processed femurs and L4s were performed by Yale Core Center for Musculoskeletal Disorders (New Haven, CT).

Gene Expression

Dissected tissues were frozen immediately in liquid nitrogen, and stored at −80°C. Frozen tissues were homogenized in Trizol Reagent (Life technologies, Grand Island, NY) and RNA was isolated according to the manufacturer's instructions. Lymphocytes were isolated and their RNA was recovered as previously described [34]. RNA (1μg) was used as a template to synthesize cDNA using the High-Capacity cDNA Reverse Transcription Kit (Applied Biosystems, Foster City, CA). RNA isolation and cDNA production was performed in a blinded fashion. Relative mRNA levels were determined via multiplex TaqMan quantitative reverse transcription-PCR (RT-PCR) using VIC labeled Mouse ACTB and FAM labeled TaqMan gene expression assays (Applied Biosystems, Foster City, CA). The following TaqMan Gene Expression probes (Applied Biosystems, Foster City, CA) were used for RT-PCR: RANKL (*Tnfsf11*, Mm00441906), CtsK (*Ctsk*, Mm00484039), OPG (*Tnfrsf11b*, Mm01205928), IL-6 (*Il6*, Mm00446190), *Cyp27b1* (Mm01165918), *Cyp24a1* (Mm00487244) and mouse ACTB (*Actb*, 4352341E). Relative mRNA levels were calculated using the ΔCt method [35].

Blood chemistry

Cardiac blood was collected at the time of sacrifice. Collected blood was maintained at room temperature for 30 minutes followed by centrifugation at 6000 rpm for 12 minutes to obtain serum. Soluble RANKL (sRANKL) content in the serum was measured using an R&D Systems Quantikine Mouse RANKL kit (Cat. No. MTR00) according to the manual provided by the manufacturer. Serum calcium was measured using Bioassay Systems QuantiChrom™ Calcium Assay Kit (Cat. No. DICA-500). Bone related degradation products from C-terminal telopeptides of type I collagen (CTX-I) and collagen type I propeptide (P1NP) were measured in serum using RatLaps™ CTX-I (Cat. No. AC-06F1) and Rat/Mouse P1NP assay (Cat. No. AC-33F1) according to the manufacturer's directions. Cardiac blood was collected in 0.5M EDTA containing tubes and plasma was isolated by

centrifugation at 6000 rpm for 12 minutes. Plasma parathyroid hormone (PTH) levels were measured using a mouse PTH (1–84) ELISA kit (Cat. No. 60-2305, Immutopics, San Clemente, CA) according to the manufacturer's directions.

Statistical Evaluation

Data were analyzed using GraphPad Prism 4 software (GraphPad Software, Inc., La Jolla, CA). All values are reported as the mean ± standard deviation (S.D.) and differences between group means were evaluated using Two-Way ANOVA or Student's *t*-test as indicated in the figure legends. To determine if the differences in RANKL mRNA levels (Fig. 3) or BMDs (Fig. 6) between the wild type and knockout mice increase with age, we performed two factor factorial with interactions using SAS software (SAS Institute Inc., Cary, NC).

RESULTS

VDR, RXR or pCREB bind RL-D2 in an inducible manner

We previously employed ChIP-chip analysis in ST2 osteoblasts using antibodies to VDR and RXR to identify six distal enhancers of *Tnfsf11* termed RL-D1 to RL-D5 and RL-D7 (Fig. 1A) [19]. Subsequent direct ChIP analysis using antibodies to phosphorylated CREB (pCREB) revealed that this transcription factor also bound strongly to RL-D2 and RL-D5 [21,29]. Further examination of the RL-D5 region via transcriptional reporters or BAC deletion methodologies showed that this enhancer was an important regulator of RANKL expression in response to $1,25(OH)_2D_3$ and PTH [19,21,24,29]. Examination of the RL-D2 region with similar methodologies; however, showed little to no regulation of RANKL by this region. Based upon these studies, we queried ChIP-seq analyses performed previously in the pre-osteoblast cell line MC3T3-E1 [32,33] to confirm our previous findings. As is seen in Figure 1B, VDR and RXR bound to five of the previously identified enhancers, namely RL-D2 to RL-D5 and RL-D7, in response to $1,25(OH)_2D_3$ in MC3T3-E1 cells. ChIP-seq analysis in the MC3T3-E1 cell line also showed that upon forskolin treatment, pCREB bound to three of the previously identified RANKL enhancers, namely RL-D2, RL-D4 and RL-D5, confirming our earlier findings in ST2 cells (Fig. 1C).

RL-D2 participates in PTH and $1,25(OH)_2D_3$ regulation of RANKL

In order to determine whether RL-D2 plays a role in transcriptional regulation of *Tnfsf11*, we removed this enhancer from the mouse genome using standard methods of homologous recombination. We then isolated bone marrow from RL-D2 enhancer deleted (D2KO) mice as well as RL-D5 enhancer deleted (D5KO) mice and their corresponding wild type (WT) littermates (D2WT or D5WT), and differentiated the adherent stromal cell populations ex vivo into osteoblast-like cells. Both, D5KO and D2KO cells expressed significantly less RANKL compared to their wild type controls (Fig. 2A). Twenty four hour treatment of these differentiated stromal cells with oncostatin M (OSM) and forskolin (Fsk), but not $1,25(OH)_2D_3$, increased interleukin 6 (IL-6) expression to similar levels in cultured D5KO or D2KO cells and their WT controls (Sup. Fig. 1A), suggesting that all cells were differentiated and treated similarly. As has previously been reported [29,30], lack of RL-D5 blunted the OSM-, Fsk- and $1,25(OH)_2D_3$-induced increase in RANKL expression (Fig.

2A). However, lack of RL-D2 blunted only Fsk- and $1,25(OH)_2D_3$-induced increases in RANKL expression (Fig. 2A).

To determine whether RL-D2 regulates RANKL expression in response to PTH and $1,25(OH)_2D_3$ in vivo, we injected 8-week-old female D2KO mice and their control littermates with a single dose of either PTH or $1,25(OH)_2D_3$. Expression of RANKL was measured 1 hr after PTH injection and 6 hrs after $1,25(OH)_2D_3$ injection. PTH injection increased control IL-6 mRNA levels and $1,25(OH)_2D_3$ decreased OPG mRNA levels similarly in all mouse strains, suggesting equivalent injection in all genotypes (Sup. Fig. 1B, C). As can be seen in Figure 2B, lack of RL-D2 significantly blunted the PTH-induced increase in RANKL mRNA in bone marrow and bones of D2KO mice. However, we were unable to detect a blunting of the $1,25(OH)_2D_3$-induced RANKL expression in D2KO bone marrow or in any of the D2KO bones measured (Fig. 2C). These results suggest that RL-D2 plays a significant role in induction of RANKL expression by PTH; however, its contribution to $1,25(OH)_2D_3$ induction of RANKL expression in vivo appears limited.

Lack of RL-D2 leads to lower skeletal RANKL expression

We then measured RANKL mRNA levels in several bones, lymphoid tissues, and bone marrow of D2KO mice and their control littermates up to 48 weeks (w) of age. At 5w of age RANKL expression in D2KO mice was similar to that of their littermate controls in all tissues measured (S. Fig. 2A). In contrast, skeletal RANKL expression in D2KO males at 8w was significantly lower compared to littermate controls (Fig. 3A). However, only vertebral RANKL was lower than WT controls in female D2KO mice (Fig. 3B). Animals that lack RL-D5 also displayed a 20–40% decrease in bone RANKL expression at 20w as previously reported [30]. Similar to D5KO mice, RANKL mRNA levels in tibia, vertebra, and femur shafts of D2KO mice of both sexes were 20–40% lower compared to the WT controls at 24w (Fig. 3C, D) and 30–50% lower compared to the WT controls at 48 w (Fig. 3E, F). Interestingly the difference in RANKL mRNA levels at 24w and 48w was most pronounced in D2KO femur shafts enriched in osteoblasts and osteocytes (Fig. 3C–F). These results suggest that RL-D2 contributes to RANKL expression in bone and especially in osteoblasts and osteocytes.

Spleen and thymus RANKL mRNA levels in D5KO mice were 50% and 25% lower compared to littermate controls at 1 and 5 months (m) of age, respectively [30]. Unlike D5KO mice, D2KO mice did not show decreased thymus RANKL mRNA levels at any age (S. Fig. 2A, Fig. 3A–F), although a 20–30% decrease in spleen RANKL expression was observed at 48w of age (Fig. 3E–F). In addition, RANKL expression in the bone marrow of D2KO mice was 30–40% lower than littermate controls at all ages measured (Fig. 3A–F). In order to determine if lower RANKL expression levels in spleen and bone marrow of D2KO mice were a result of loss of RL-D2 mediated control of lymphocyte RANKL expression, we isolated lymphocytes from bone marrow and spleens of 24w old female D2KO mice and measured RANKL mRNA levels. As can be seen from S. Fig. 3, lack of RL-D2 did not alter RANKL mRNA levels in either T or B cells. These results suggest that RL-D2 participates in RANKL expression in spleen and bone marrow**,** perhaps by contributing to RANKL expression of mesenchymal lineage cells residing within these tissues.

D2KO mice have decreased bone remodeling

Osteocyte RANKL has been shown to be the functional source of RANKL supporting osteoclast formation in adult bones [9]. Since lack of RL-D2 decreased RANKL expression significantly in femur shafts of D2KO mice (Fig. 3A–F), we next assessed whether the decrease in RANKL expression in these mice affected osteoclast formation. As shown in Fig. 4A–E and consistent with lower RANKL levels, mRNA levels of osteoclast marker gene *Cathepsin K* (CtsK) were lower in the bones of D2KO mice, suggesting that these enhancer deleted mice displayed lower osteoclast numbers. Despite the strong reduction in RANKL expression in 48w old female D2KO mice, a decrease in CtsK mRNA levels was not significant (Fig. 4F); however, this may be due to the low animal numbers examined at this age.

Consistent with the decrease in osteoclast maker gene CtsK, D2KO mice had lower circulating levels of collagen type 1 cross-linked C-telopeptide (CTX-I) compared to their littermate controls (Fig. 5B). Moreover, due to coupling between bone resorption and formation, D2KO mice also manifested lower bone formation represented by a decrease in circulating levels of type 1 procollagen (N-terminal) (PN1P) levels (Fig. 5C). Taken together, our results suggest that D2KO mice exhibit decreased bone resorption leading to decreased bone remodeling. Interestingly, despite the decreased bone resorption and thus, decreased release of calcium from the skeletal stores, D2KO mice retain serum calcium levels similar to that of their wild type littermates (Fig. 5D). Consistent with the observations in D5KO mice, wild type and D2KO mice have similar plasma PTH levels (Fig. 5E). Moreover, kidney mRNA levels of 1α-hydroxylase (*Cyp27b1*), which synthesizes the active form of vitamin D_3, and *Cyp24a1,* which initiates the degradation of active form of vitamin D_3 (Figure 5F, G), are similar in wild type and D2KO mice. Together, these results suggest that intestinal absorption and renal reabsorption of calcium are adequate to maintain calcium homeostasis of D2KO mice under basal conditions.

Mice lacking RL-D2 have high bone mass phenotype specific to the cancellous compartment

To determine potential changes in bone mass of D2KO mice, the bone mineral density (BMD) of these enhancer deleted mice and their wild type littermate controls were measured at 5, 8, 24 and 48 weeks of age. At all time points, the body weights of the D2KO mice and their control littermates were similar (S. Fig. 2C, D). It has been shown that at 1m of age, female D5KO mice have higher vertebral BMD [12,30]. However, this parameter in female D2KO mice was not different from controls at any of the sites measured (S. Fig. 2B). In contrast, by 8w the BMD of both male and female D2KO mice was statistically higher than that of their wild type littermate controls in a fashion analogous to that of D5KO mice (Fig. 6A, D)[12,30]. Importantly, BMD differences between D2KO mice and D2WT mice of both sexes became more pronounced with age (Fig. 6B, C, E and F) and statistical comparison of the difference between WT and D2KO mice utilizing two factor factorial with interactions suggested that the skeletal phenotype of D2KO mice progresses in an age dependent manner. D5KO mice have also been shown to exhibit higher cancellous bone volume without changes to cortical bone [12]. Similar to the D5KO mice and in agreement with the BMD data, μCt analysis at 12 months of age showed an increase in cancellous bone volume in

femur and spine of D2KO animals (Fig. 7A, E, F and K). Consistent with decreased bone remodeling in the cancellous bone compartment, the increased cancellous bone volume of the D2KO mice was associated with increased trabecular number (Fig. 7B, G) and decreased trabecular spacing (Fig. 7C, H) without a change in trabecular thickness (Fig. 7D, I). Moreover, as with D5KO mice [12], cortical thickness at the femoral midshafts was nevertheless similar in both D2KO and D2WT mice (Fig. 7J, L). Together, these results suggest that lack of RL-D2 leads to decreased bone remodeling in the cancellous bone compartment causing increased cancellous bone volume without an effect on cortical bone.

Lack of RL-D2 does not alter pCREB binding to RL-D4 or RL-D5

We have recently shown that lack of an enhancer can alter transcription factor binding to other enhancers that coregulate the same gene [36]. ChIP-seq analysis has shown that Fsk treatment induces pCREB binding to RL-D2, RL-D4 and RL-D5 (Fig. 1C). Because both RL-D2 and RL-D5 regulate RANKL expression via PTH and mice that lack either of these enhancers have similar phenotypes, we asked whether RL-D2 might regulate PTH induction of RANKL, at least in part, through enhancer interaction by altering pCREB binding to RL-D5. Bone marrow was isolated from femurs and humeri of WT and D2KO mice and then differentiated to an osteoblastic phenotype ex vivo in osteogenic medium. These cells express RANKL in a PTH-, Fsk- and $1,25(OH)_2D_3$-inducible manner (Fig. 2 and data not shown). The differentiated primary cells were then treated with vehicle or Fsk for 1 hr and ChIP analysis was performed using the pCREB antibody. Quantitative RT-PCR utilizing primers within the RL-D2 region showed inducible pCREB binding in wild type cells; ChIP signal for the DNA segment corresponding to RL-D2 was absent in D2KO cells, confirming this regions' absence in the D2KO mice from which they were obtained (Fig. 8B). Consistent with the ChIP-seq data on osteoblastic MC3T3 cells (Fig. 1C), Fsk treatment induced pCREB binding specifically to RL-D2, RL-D4 and RL-D5 in the wild type cells (Fig. 8 B–D), but not in negative control region (−30k region of *Mmp13* gene) (Fig. 8A). However, basal and inducible pCREB binding was not altered in cells that lacked RL-D2 (Fig. 8 B–D), suggesting that the phenotype of the D2KO mice is not due to alterations in pCREB binding to RL-D4 or RL-D5. It is worth noting that basal pCREB binding is higher in direct ChIP-qPCR than in ChIP-seq assessments, due in part to an increase in sensitivity in the former assay. The conclusion, however, is identical in both cases.

DISCUSSION

Recent advances in genome wide studies have significantly altered our understanding of the regulatory landscapes of most genes. We now know that many genes are regulated through multiple enhancers that are frequently located several kilobases distant from their transcriptional start sites and interact not only with promoters but with each other as well to orchestrate transcriptional regulation [37–39]. *Tnfsf11* represents a classic example of this type of complex transcriptional regulation. Previous studies in our laboratory and others have led to the identification of ten *Tnfsf11* enhancers that are located up to 155 kb upstream of the gene's TSS [19–24,28,29]. One of the *Tnfsf11* enhancers termed RL-D5 and located 76 kb upstream of the gene's TSS represents a multifunctional enhancer that mediates RANKL expression in response to PTH, $1,25(OH)_2D_3$ and IL-6-type cytokines [19,29]. Herein, we

show that RL-D2, which is located 23 kb upstream of the *Tnfsf11* TSS, also mediates PTH-induction of RANKL expression in *cis*. Lack of either RL-D2 or RL-D5 blunts the PTH-induced increase in RANKL expression in vivo, suggesting that both RL-D2 and RL-D5 contribute to the PTH-modulated increase in RANKL transcription. Consistent with this finding and the concept that PTH plays a central and ambient role in regulating bone remodeling, mice that lack RL-D2 exhibit lower RANKL mRNA levels in bones, bone marrow, and spleen. Importantly, lower RANKL mRNA levels in D2KO mice are associated with decreased osteoclast numbers and bone resorption as indicated by decreased osteoclast marker gene expression and circulating bone resorption markers. Similar to the previous observation in RL-D5 null mice [12,30], D2KO mice exhibit a progressive increase in bone mass beginning at 8w of age. This increase in bone mass in D2KO mice is due to changes in cancellous bone architecture without a change in cortical bone thickness. These results together with previous findings in D5KO mice indicate that RL-D2 and RL-D5 play overlapping roles in the regulation of *Tnfsf11* expression by PTH, and allow a prediction that deletion of both enhancers might fully compromise PTH action in *Tnfsf11* expression.

In addition to mediating PTH regulation of RANKL, ChIP and ChIP-seq analyses in multiple osteoblast or pre-osteoblast cell lines have shown that VDR and RXR bind to RL-D2 in an inducible manner [19,32], suggesting a role for RL-D2 in mediating $1,25(OH)_2D_3$ induction of RANKL. Consistent with this observation, lack of RL-D2 blunted the $1,25(OH)_2D_3$-induced increase in RANKL expression in ex vivo stromal cell cultures. However, we were unable to detect a blunting of the $1,25(OH)_2D_3$ induction of RANKL in vivo. This may be due to the role of RL-D2 in mediating the $1,25(OH)_2D_3$ response of RANKL in a small population of cells that do not contribute to a significant increase in RANKL expression observed in whole bone. Alternatively, the role of RL-D2 in mediating the activity of $1,25(OH)_2D_3$ on RANKL expression may be restricted temporally or spatially to specific skeletal or other sites or limited hierarchically to accelerated bone resorption contexts characteristic of prolonged dietary calcium deficiency or other specific disease states.

With current advances in genome-wide analysis of transcription factor binding, DNase I hypersensitivity, histone modifications and DNA methylation, it has becoming quite clear that most genes are regulated through multiple enhancers [37–40]. Several models have been proposed to explain the mechanisms through which groups of enhancers may work together to regulate gene expression [41,42]. One such model suggests the looping of the DNA to bring multiple enhancers at a locus together with the gene promoters they regulate to mediate transcription [41]. Using chromatin conformation capture (3C) assays, we have confirmed at several transcriptional loci including that of *Cyp24a1*[43] and *Mmp13* [36] that distant enhancers converge at their respective promoters to allow transcriptional control of these genes. Interestingly, we have recently shown that the deletion of one of several enhancers that controls *Mmp13* expression can alter transcription factor binding at other enhancers in this transcriptional locus and their activities as well [36]. We show here, however, that both basal and PTH-inducible pCREB binding at the *Tnfsf11* enhancers RL-D4 and RL-D5 enhancers is unaffected by deletion of the RL-D2 enhancer. Since deletion of RL-D2 or RL-D5 results in a reduction in PTH-sensitive RANKL induction in both enhancer deleted mouse strains, these data support the idea that these two enhancers perform

an additive rather than cooperative or synergistic function to regulate PTH mediated expression of *Tnfsf11*. It is important to note, however, that our results represent only binding and not activity measurements, and we have not determined at this point whether these enhancers influence each other's activity(s) or whether their multiple activities are integrated at the level of the *Tnfsf11* promoter. Thus, it remains of considerable interest to identify the mechanisms through which the multiple RANKL enhancers co-regulate expression of the *Tnfsf11* gene.

RANKL is expressed in a wide range of cell types including, but not limited to, osteoblast-lineage cells and lymphocytes. We have recently shown that a DNA segment spanning 46 kb downstream to 178 kb upstream of the *Tnfsf11* TSS is capable of producing RANKL mRNA in a cell-type specific fashion in vivo [34]. Our genome-wide studies using cell lines from mesenchymal and hematopoietic lineages have suggested that while RL-D5 is an enhancer active in both of these lineages, other enhancers such as RL-T1 or RL-D2 are each active only in one of the two lineages [19,20,23]. Consistent with our genome-wide in vitro studies, mice that lack RL-D5 have a 50% decrease in spleen and a 25% decrease in thymus RANKL expression [30], due in part to lower RANKL expression in lymphocytes [44]. However, in this study we show that the decrease in splenic RANKL expression (25–30%) in the RL-D2 enhancer deleted mice is much less than that observed in spleen tissues from D5KO mice, an effect that is not due to a reduction in lymphocyte RANKL expression. Moreover, unlike D5KO mice, thymic RANKL expression remains unaltered in D2KO mice. We also show that the lower RANKL levels seen in bone marrow or spleens of D2KO mice are not due to decreased lymphocyte RANKL. These results suggest that RL-D2 is indeed inactive in hematopoietic lineage cells and that the lower RANKL expression in these tissues is likely due to lower synthesis of RANKL expression in mesenchymal lineage cells that reside within these tissues.

As previously mentioned, it is known that the functional source of RANKL during growth is the chondrocyte and during adulthood is the osteocyte [9,10]. The most striking decrease in RANKL levels in D2KO mice was observed in femur shafts enriched in osteoblasts and osteocytes (up to 60% decrease). While it is possible that RL-D2 may contribute to hypertrophic chondrocyte RANKL transcription, the fact that the significant decrease in skeletal RANKL levels and the resultant high bone mass phenotype becomes evident at only 8w of age and that this phenotype progresses with age, suggests that altered RANKL expression in chondrocytes in D2KO and D5KO mice may not be significant. Thus, it is more likely that RL-D2 is responsible for mediating RANKL expression in osteocytes rather than chondrocytes. While transcriptional control of this physiologically relevant source of RANKL is very important, it is not possible currently, due to technical restraints to determine the contribution of these RANKL enhancers to hypertrophic chondrocyte expression in vivo. On the other hand, ex vivo cultures of primary chondrocytes or transformed chondrocyte cell lines such as ATDC5 [45], that go under hypertrophy, could represent important resources in understanding the regulation of chondrocyte RANKL expression in the future.

RANKL is produced as a transmembrane protein that can be cleaved into a soluble form [46,47]. While measuring soluble RANKL (sRANKL) is a common practice in

pathological conditions, the source or the physiological importance of the soluble form of RANKL is unknown. It has previously been shown that animals that lack osteocyte and osteoblast RANKL have normal levels of circulating sRANKL [9]. As seen herein, circulating sRANKL is unchanged in D2KO mice as well (Fig. 5A). However, all mouse strains that lack osteocyte RANKL[9] or RL-D2 regulation of RANKL have high bone mass phenotypes. These results suggest that mesenchymal cells are not a significant source of circulating sRANKL and point to the importance of local production of membrane-bound RANKL.

Overall, the results described herein indicate that the RL-D2 and RL-D5 enhancers exhibit both overlapping as well as distinct functional roles in the regulation of RANKL expression, particularly as they relate to mediating the activity of PTH on this gene. Given the individual common role of both of these enhancers, we speculate that simultaneous deletion of both enhancers would likely lead to complete abrogation of PTH regulation of this gene in vivo. Recent studies provide data suggesting that PTH may regulate RANKL expression via an element located 1 to 2 kb upstream of the *Tnfsf11* promoter [48]. While it is possible that PTH action may occur independent of CREB activation [49,50], as suggested in this specific report by Obri et al., this finding is in contrast to earlier studies that have shown that the activation of CREB is indeed central to the induction of *Tnfsf11* by PTH [51–53]. Thus, it is noteworthy that pCREB binding in our ChIP-seq analyses was neither present nor induced by forskolin within the interval between the *Tnfsf11* promoter and its upstream RL-D2 enhancer located at −23 kb (Fig. 1C). Additional studies have shown that a number of other RANKL regulators also modulate the expression of this gene through promoter proximal elements [45,54–56]. Unfortunately, none of these activities have been confirmed using more recent unbiased ChIP-seq analyses together with more contemporary enhancer methodologies. Interestingly, we have recently observed that CRISPR/Cas9 mediated deletion of the mouse *Tnfsf11* gene region from −0.5 kb to −8 kb in osteoblastic cells had no effect on PTH, $1,25(OH)_2D_3$, or IL-6 mediated regulation of RANKL expression (Meyer, Onal, and Pike, unpublished). While this finding will require confirmation in vivo, we argue that traditional methods that define regulation out of genomic context are prone to error and that the regulation of RANKL expression in osteoblast lineage cells is mediated exclusively through the upstream distal elements that we have defined. Regardless, our results confirm and extend our understanding of the functional roles of two distal enhancers for the *Tnfsf11* gene in vivo.

In summary, both RL-D2 and RL-D5 are required for the PTH regulation of RANKL transcription and lack of either of these enhancers causes a decrease in bone remodeling that leads to a high bone mass phenotype. While RL-D5 is a multifunctional enhancer that is active in multiple lineages, PTH and $1,25(OH)_2D_3$ regulation of RANKL transcription through RL-D2 appears to be restricted to cells of the mesenchymal lineage. These results highlight the complex nature of RANKL transcriptional control and point out the importance of identifying the physiological roles of unique gene enhancers in vivo.

Supplementary Material

Refer to Web version on PubMed Central for supplementary material.

Acknowledgments

We thank members of the Pike laboratory especially Jon W. Markert, Erin M. Riley, Nancy A. Benkusky and Mark B. Meyer for their contributions to this work, and Peter Crump for his help with statistical analysis. We also thank members of the UW Biochemistry Animal Support Staff for their contributions to this effort.

References

1. Kong YY, Yoshida H, Sarosi I, et al. OPGL is a key regulator of osteoclastogenesis, lymphocyte development and lymph-node organogenesis. Nature. 1999; 397(6717):315–23. [PubMed: 9950424]
2. Kim D, Mebius RE, MacMicking JD, et al. Regulation of peripheral lymph node genesis by the tumor necrosis factor family member TRANCE. J Exp Med. 2000; 192(10):1467–78. [PubMed: 11085748]
3. Hess E, Duheron V, Decossas M, et al. RANKL induces organized lymph node growth by stromal cell proliferation. J Immunol. 2012; 188(3):1245–54. [PubMed: 22210913]
4. Hanada R, Leibbrandt A, Hanada T, et al. Central control of fever and female body temperature by RANKL/RANK. Nature. 2009; 462(7272):505–9. [PubMed: 19940926]
5. Onal M, Xiong J, Chen X, et al. Receptor activator of nuclear factor κB ligand (RANKL) protein expression by B lymphocytes contributes to ovariectomy-induced bone loss. J Biol Chem. 2012; 287(35):29851–60. [PubMed: 22782898]
6. Fata J, Kong Y, Li J, et al. The osteoclast differentiation factor osteoprotegerin-ligand is essential for mammary gland development. Cell. 2000; 103(1):41–50. [PubMed: 11051546]
7. Lacey D, Timms E, Tan H, et al. Osteoprotegerin ligand is a cytokine that regulates osteoclast differentiation and activation. Cell. 1998; 93(2):165–76. [PubMed: 9568710]
8. Kim N, Odgren PR, Kim DK, Marks SC, Choi Y. Diverse roles of the tumor necrosis factor family member TRANCE in skeletal physiology revealed by TRANCE deficiency and partial rescue by a lymphocyte-expressed TRANCE transgene. Proc Natl Acad Sci U S A. 2000; 97(20):10905–10. [PubMed: 10984520]
9. Xiong J, Onal M, Jilka RL, Weinstein RS, Manolagas SC, O'Brien CA. Matrix-embedded cells control osteoclast formation. Nat Med. 2011; 17(10):1235–41. [PubMed: 21909103]
10. Nakashima T, Hayashi M, Fukunaga T, et al. Evidence for osteocyte regulation of bone homeostasis through RANKL expression. Nat Med. 2011; 17(10):1231–4. [PubMed: 21909105]
11. O'Brien C, Jilka R, Fu Q, Stewart S, Weinstein R, Manolagas S. IL-6 is not required for parathyroid hormone stimulation of RANKL expression, osteoclast formation, and bone loss in mice. Am J Physiol Endocrinol Metab. 2005; 289(5):E784–93. [PubMed: 15956054]
12. Onal M, Galli C, Fu Q, et al. The RANKL distal control region is required for the increase in RANKL expression, but not the bone loss, associated with hyperparathyroidism or lactation in adult mice. Mol Endocrinol. 2012; 26(2):341–8. [PubMed: 22207718]
13. Kong YY, Feige U, Sarosi I, et al. Activated T cells regulate bone loss and joint destruction in adjuvant arthritis through osteoprotegerin ligand. Nature. 1999; 402(6759):304–9. [PubMed: 10580503]
14. Komatsu N, Takayanagi H. Autoimmune arthritis: the interface between the immune system and joints. Adv Immunol. 2012; 115:45–71. [PubMed: 22608255]
15. Kitazawa R, Kitazawa S. Vitamin D(3) augments osteoclastogenesis via vitamin D-responsive element of mouse RANKL gene promoter. Biochem Biophys Res Commun. 2002; 290(2):650–5. [PubMed: 11785948]
16. Kitazawa S, Kajimoto K, Kondo T, Kitazawa R. Vitamin D3 supports osteoclastogenesis via functional vitamin D response element of human RANKL gene promoter. J Cell Biochem. 2003; 89(4):771–7. [PubMed: 12858342]
17. Ernst J, Kheradpour P, Mikkelsen TS, et al. Mapping and analysis of chromatin state dynamics in nine human cell types. Nature. 2011; 473(7345):43–9. [PubMed: 21441907]
18. Ram O, Goren A, Amit I, et al. Combinatorial patterning of chromatin regulators uncovered by genome-wide location analysis in human cells. Cell. 2011; 147(7):1628–39. [PubMed: 22196736]

19. Kim S, Yamazaki M, Zella L, Shevde N, Pike J. Activation of receptor activator of NF-kappaB ligand gene expression by 1,25-dihydroxyvitamin D3 is mediated through multiple long-range enhancers. Mol Cell Biol. 2006; 26(17):6469–86. [PubMed: 16914732]
20. Kim S, Yamazaki M, Zella LA, et al. Multiple enhancer regions located at significant distances upstream of the transcriptional start site mediate RANKL gene expression in response to 1,25-dihydroxyvitamin D3. J Steroid Biochem Mol Biol. 2007; 103(3–5):430–4. [PubMed: 17197168]
21. Kim S, Yamazaki M, Shevde N, Pike J. Transcriptional control of receptor activator of nuclear factor-kappaB ligand by the protein kinase A activator forskolin and the transmembrane glycoprotein 130-activating cytokine, oncostatin M, is exerted through multiple distal enhancers. Mol Endocrinol. 2007; 21(1):197–214. [PubMed: 17053039]
22. Martowicz ML, Meyer MB, Pike JW. The mouse RANKL gene locus is defined by a broad pattern of histone H4 acetylation and regulated through distinct distal enhancers. J Cell Biochem. 2011; 112(8):2030–45. [PubMed: 21465526]
23. Bishop KA, Coy HM, Nerenz RD, Meyer MB, Pike JW. Mouse Rankl expression is regulated in T cells by c-Fos through a cluster of distal regulatory enhancers designated the T cell control region. J Biol Chem. 2011; 286(23):20880–91. [PubMed: 21487009]
24. Nerenz RD, Martowicz ML, Pike JW. An enhancer 20 kilobases upstream of the human receptor activator of nuclear factor-kappaB ligand gene mediates dominant activation by 1,25-dihydroxyvitamin D3. Mol Endocrinol. 2008; 22(5):1044–56. [PubMed: 18202151]
25. Bishop KA, Wang X, Coy HM, Meyer MB, Gumperz JE, Pike JW. Transcriptional regulation of the human TNFSF11 gene in t cells via a cell type-selective set of distal enhancers. J Cell Biochem. 2014; 116(2):320–30. [PubMed: 25211367]
26. Onal M, Bishop KA, St John HC, et al. A DNA Segment Spanning the Mouse Tnfsf11 Transcription Unit and Its Upstream Regulatory Domain Rescues the Pleiotropic Biologic Phenotype of the RANKL Null Mouse. J Bone Miner Res. 2014; 30(5):855–68. [PubMed: 25431114]
27. Kim S, Yamazaki M, Zella L, et al. Multiple enhancer regions located at significant distances upstream of the transcriptional start site mediate RANKL gene expression in response to 1,25-dihydroxyvitamin D_3. J Steroid Biochem Mol Biol. 2007; 103(3–5):430–4. [PubMed: 17197168]
28. Bishop KA, Wang X, Coy HM, Meyer MB, Gumperz JE, Pike JW. Transcriptional regulation of the human TNFSF11 gene in t cells via a cell type-selective set of distal enhancers. J Cell Biochem. 2014 In Press.
29. Fu Q, Manolagas S, O'Brien C. Parathyroid hormone controls receptor activator of NF-kappaB ligand gene expression via a distant transcriptional enhancer. Mol Cell Biol. 2006; 26(17):6453–68. [PubMed: 16914731]
30. Galli C, Zella L, Fretz J, et al. Targeted deletion of a distant transcriptional enhancer of the receptor activator of nuclear factor-kappaB ligand gene reduces bone remodeling and increases bone mass. Endocrinology. 2008; 149(1):146–53. [PubMed: 17932217]
31. Meyer MB, Goetsch PD, Pike JW. VDR/RXR and TCF4/β-catenin cistromes in colonic cells of colorectal tumor origin: impact on c-FOS and c-MYC gene expression. Mol Endocrinol. 2012; 26(1):37–51. [PubMed: 22108803]
32. St John HC, Meyer MB, Benkusky NA, et al. The parathyroid hormone-regulated transcriptome in osteocytes: Parallel actions with 1,25-dihydroxyvitamin D3 to oppose gene expression changes during differentiation and to promote mature cell function. Bone. 2014; 72C:81–91. [PubMed: 25460572]
33. Meyer MB, Benkusky NA, Lee CH, Pike JW. Genomic determinants of gene regulation by 1,25-dihydroxyvitamin D3 during osteoblast-lineage cell differentiation. J Biol Chem. 2014; 289(28): 19539–54. [PubMed: 24891508]
34. Onal M, Bishop KA, St John HC, et al. A DNA Segment Spanning the Mouse Tnfsf11 Transcription Unit and Its Upstream Regulatory Domain Rescues the Pleiotropic Biologic Phenotype of the RANKL Null Mouse. J Bone Miner Res. 2014
35. Livak KJ, Schmittgen TD. Analysis of relative gene expression data using real-time quantitative PCR and the 2(−Delta Delta C(T)) Method. Methods. 2001; 25(4):402–8. [PubMed: 11846609]

36. Meyer MB, Benkusky NA, Pike JW. Selective Distal Enhancer Control of the Mmp13 Gene Identified through Clustered Regularly Interspaced Short Palindromic Repeat (CRISPR) Genomic Deletions. J Biol Chem. 2015; 290(17):11093–107. [PubMed: 25773540]
37. Smith E, Shilatifard A. Enhancer biology and enhanceropathies. Nat Struct Mol Biol. 2014; 21(3): 210–9. [PubMed: 24599251]
38. Neph S, Vierstra J, Stergachis AB, et al. An expansive human regulatory lexicon encoded in transcription factor footprints. Nature. 2012; 489(7414):83–90. [PubMed: 22955618]
39. Sanyal A, Lajoie BR, Jain G, Dekker J. The long-range interaction landscape of gene promoters. Nature. 2012; 489(7414):109–13. [PubMed: 22955621]
40. Bulger M, Groudine M. Functional and mechanistic diversity of distal transcription enhancers. Cell. 2011; 144(3):327–39. [PubMed: 21295696]
41. Bulger M, Groudine M. Looping versus linking: toward a model for long-distance gene activation. Genes Dev. 1999; 13(19):2465–77. [PubMed: 10521391]
42. Blackwood EM, Kadonaga JT. Going the distance: a current view of enhancer action. Science. 1998; 281(5373):60–3. [PubMed: 9679020]
43. Meyer MB, Goetsch PD, Pike JW. A downstream intergenic cluster of regulatory enhancers contributes to the induction of CYP24A1 expression by 1alpha,25-dihydroxyvitamin D3. J Biol Chem. 2010; 285(20):15599–610. [PubMed: 20236932]
44. Onal M, St John H, Danielson A, O'Brien CA, Pike JW. Unique Distal Enhancers Linked to the Mouse *Tnfsf11* Gene Direct Tissue-Specific Expression and Inflammation induced Regulation of RANKL Expression. J Bone Miner Res. 2014; 29(Suppl 1)
45. Usui M, Xing L, Drissi H, et al. Murine and chicken chondrocytes regulate osteoclastogenesis by producing RANKL in response to BMP2. J Bone Miner Res. 2008; 23(3):314–25. [PubMed: 17967138]
46. Lum L, Wong BR, Josien R, et al. Evidence for a role of a tumor necrosis factor-alpha (TNF-alpha)-converting enzyme-like protease in shedding of TRANCE, a TNF family member involved in osteoclastogenesis and dendritic cell survival. J Biol Chem. 1999; 274(19):13613–8. [PubMed: 10224132]
47. Kanamaru F, Iwai H, Ikeda T, Nakajima A, Ishikawa I, Azuma M. Expression of membrane-bound and soluble receptor activator of NF-kappaB ligand (RANKL) in human T cells. Immunol Lett. 2004; 94(3):239–46. [PubMed: 15275972]
48. Obri A, Makinistoglu MP, Zhang H, Karsenty G. HDAC4 integrates PTH and sympathetic signaling in osteoblasts. J Cell Biol. 2014; 205(6):771–80. [PubMed: 24934156]
49. Pfister MF, Forgo J, Ziegler U, Biber J, Murer H. cAMP-dependent and -independent downregulation of type II Na-Pi cotransporters by PTH. Am J Physiol. 1999; 276(5 Pt 2):F720–5. [PubMed: 10330054]
50. Guo J, Liu M, Yang D, et al. Phospholipase C signaling via the parathyroid hormone (PTH)/PTH-related peptide receptor is essential for normal bone responses to PTH. Endocrinology. 2010; 151(8):3502–13. [PubMed: 20501677]
51. Fu Q, Jilka RL, Manolagas SC, O'Brien CA. Parathyroid hormone stimulates receptor activator of NFkappa B ligand and inhibits osteoprotegerin expression via protein kinase A activation of cAMP-response element-binding protein. J Biol Chem. 2002; 277(50):48868–75. [PubMed: 12364326]
52. Kondo H, Guo J, Bringhurst FR. Cyclic adenosine monophosphate/protein kinase A mediates parathyroid hormone/parathyroid hormone-related protein receptor regulation of osteoclastogenesis and expression of RANKL and osteoprotegerin mRNAs by marrow stromal cells. J Bone Miner Res. 2002; 17(9):1667–79. [PubMed: 12211438]
53. Lee SK, Lorenzo JA. Regulation of receptor activator of nuclear factor-kappa B ligand and osteoprotegerin mRNA expression by parathyroid hormone is predominantly mediated by the protein kinase a pathway in murine bone marrow cultures. Bone. 2002; 31(1):252–9. [PubMed: 12110442]
54. Srivastava S, Matsuda M, Hou Z, et al. Receptor activator of NF-kappaB ligand induction via Jak2 and Stat5a in mammary epithelial cells. J Biol Chem. 2003; 278(46):46171–8. [PubMed: 12952963]

55. Roccisana J, Kawanabe N, Kajiya H, Koide M, Roodman G, Reddy S. Functional role for heat shock factors in the transcriptional regulation of human RANK ligand gene expression in stromal/osteoblast cells. J Biol Chem. 2004; 279(11):10500–7. [PubMed: 14699143]

56. Elefteriou F, Ahn J, Takeda S, et al. Leptin regulation of bone resorption by the sympathetic nervous system and CART. Nature. 2005; 434(7032):514–20. [PubMed: 15724149]

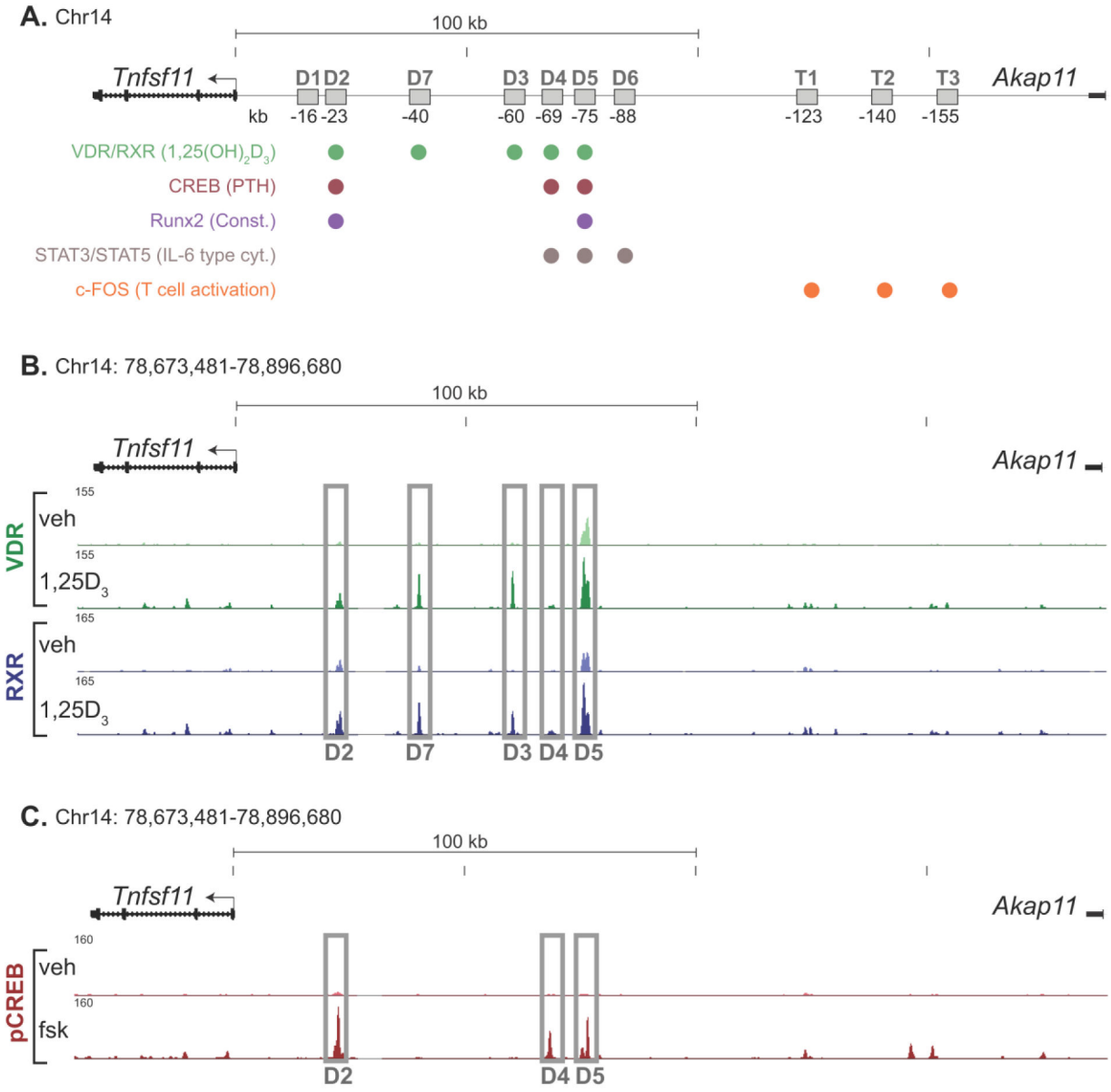

Figure 1. Transcriptional landscape of murine *Tnfsf11* gene in response to forskolin or $1,25(OH)_2D_3$ treatments in MC3T3-E1 cells

A, Schematic structure of the *Tnfsf11* gene indicating the previously identified enhancer regions (D1–D7 and T1–T3), transcription factors (pCREB, Runx2, STAT3/STAT5, and cFOS) and nuclear receptors (VDR/RXR) capable of binding to these enhancers, as well as signaling pathways stimulating these interactions (shown in parenthesis). **B**, ChIP-seq tag density (normalized to 10^7 tags) for VDR and RXR binding in MC3T3-E1 cells after 3 hrs of 10^{-7} M $1,25(OH)_2D_3$ ($1,25D_3$) or vehicle (veh) treatment. **C**, ChIP-seq tag density (normalized to 10^7 tags) for pCREB binding in MC3T3-E1 cells after 1 hr of 10^{-6} M forskolin (Fsk) or vehicle (veh) treatment.

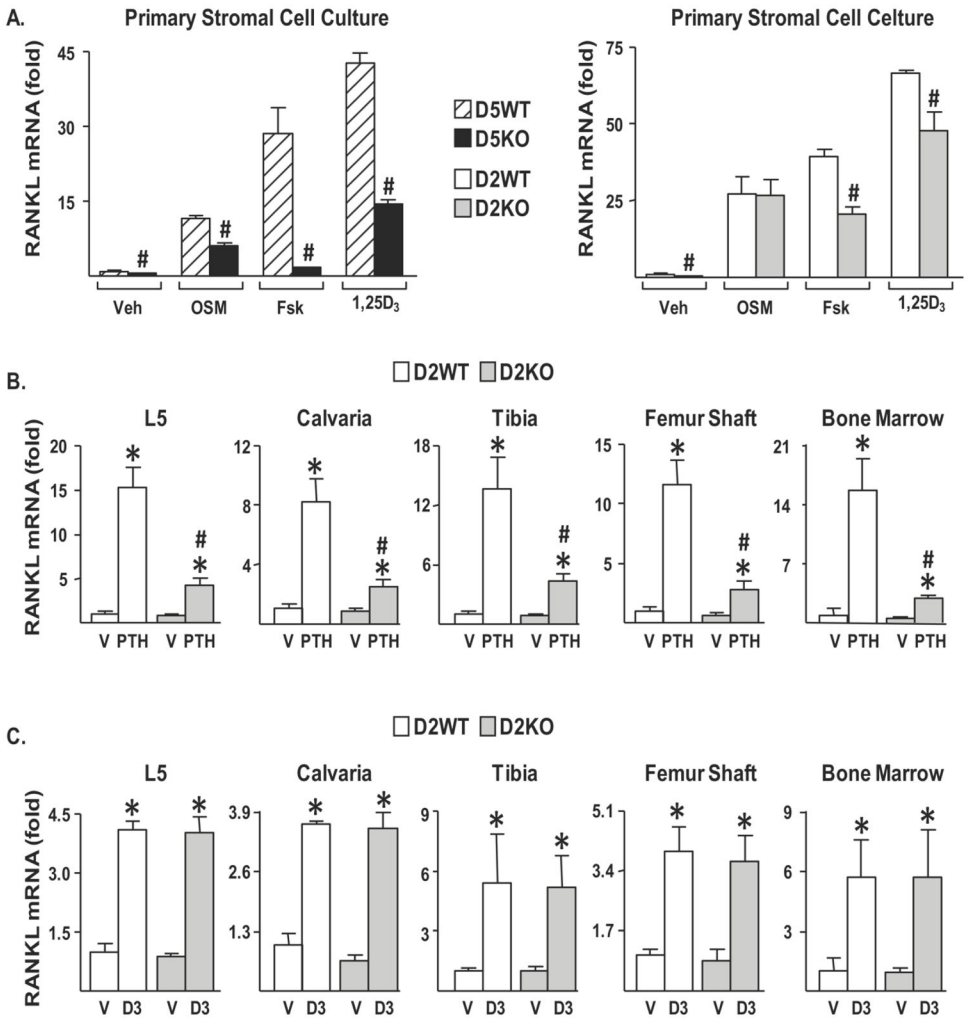

Figure 2. Fsk and PTH increase RANKL expression via RL-D2 and RL-D5 enhancers

A, Ex vivo primary stromal cultures of D5WT, D5KO, D2WT and D2KO cells were treated with vehicle (Veh), 25 ng/ml of OSM, 10^{-6} M forskolin (Fsk) or 10^{-8} M $1,25(OH)_2D_3$ ($1,25D_3$) for 24 hrs. RANKL mRNA expression in the treated cultures were measured by quantitative RT-PCR and normalized to beta-actin mRNA expression (n=3–4 wells/group). **B–C**, Eight-week-old female D2KO mice and their wild type littermates (D2WT) were injected with 230 ng/g bw of PTH (**B**) or 10 ng/g bw of $1,25(OH)_2D_3$ (D3) (**C**) or their corresponding vehicle (V). The animals were sacrificed and tissues collected 6 hrs after $1,25(OH)_2D_3$ injection or 1hr after PTH injection. **B–C**, RANKL mRNA levels in lumbar vertebra 5 (L5), calvaria, tibia, femur shafts, and bone marrow were measured by quantitative RT-PCR and normalized to beta-actin mRNA levels (n=4–6 animals/group). All values represent mean fold change relative to wild type vehicle-treated group. **A**, Statistical comparisons were accomplished using student's *t*-test. **B–C,** Statistical comparisons were accomplished using Two-Way ANOVA. *, $p<0.05$ effect of treatment within the same genotype; #, $p<0.05$ effect of genotype within the same treatment.

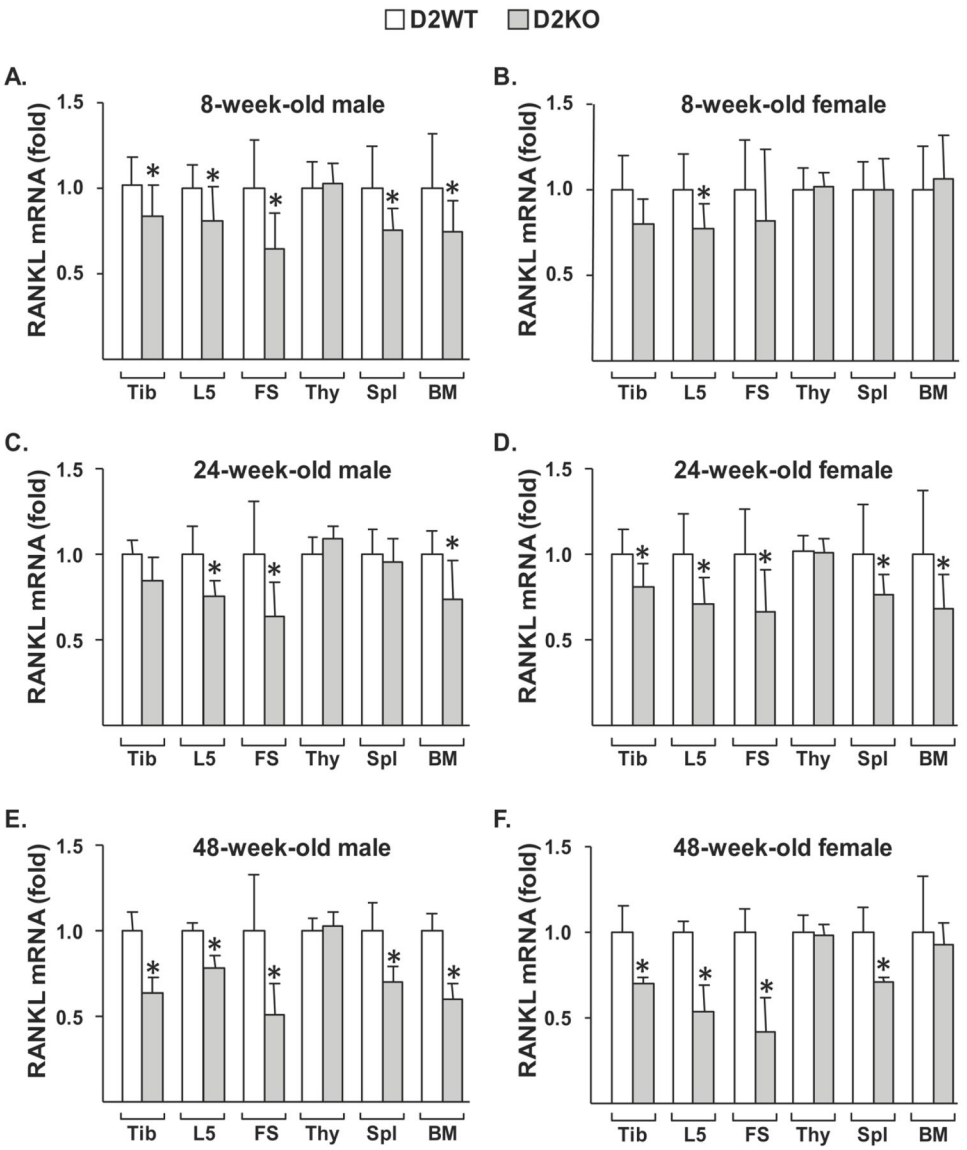

Figure 3. D2KO mice have lower RANKL expression in skeletal tissues and bone marrow

Skeletal and lymphoid tissues were collected from littermate D2WT and D2KO male (**A, C, E**) and female (**B, D, F**) mice at 8w (**A,B**), 24w (**C&D**) and 48w (**E&F**) of age. **A–F**, RANKL mRNA levels of tibia (Tib), lumbar vertebra 5 (L5), femur shafts (FS), thymus (Thy), spleen (Spl), and bone marrow (BM) were measured by quantitative RT-PCR and normalized to beta-actin mRNA levels. All values represent mean fold change relative to RANKL mRNA levels of the same tissue of D2WT group ± SD. **A–D**, At 8 and 24w of age, n=5–11 animals/group. **E–F**, At 48w of age n=3–6 animals/group. All statistical comparisons were accomplished using student's *t*-test. *, $p<0.05$ compared to wild type controls.

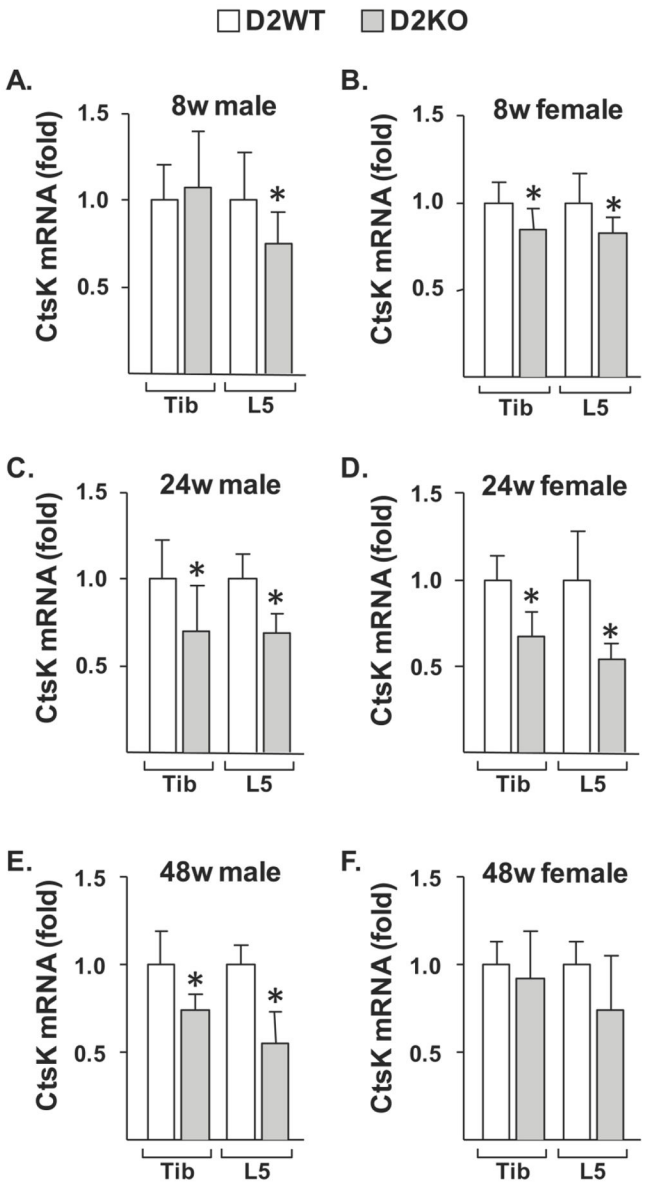

Figure 4. D2KO mice exhibit decreased osteoclast maker gene expression

Bones were collected from littermate D2WT and D2KO male (**A, C, E**) and female (**B, D, F**) mice at 8w (**A,B**), 24w (**C&D**) and 48w (**E&F**) of age. Cathepsin K (CtsK) mRNA levels in tibia (Tib) and lumbar vertebra 5 (L5) were measured by quantitative RT-PCR. All values represent mean fold change relative to CtsK mRNA levels of the D2WT group ± SD. **A–D**, At 8w and 24w of age, n=5–11 animals/group. **E–F**, At 48w of age n=3–6 animals/group. All statistical comparisons were performed using student's *t*-test. *, $p<0.05$ compared to wild type controls.

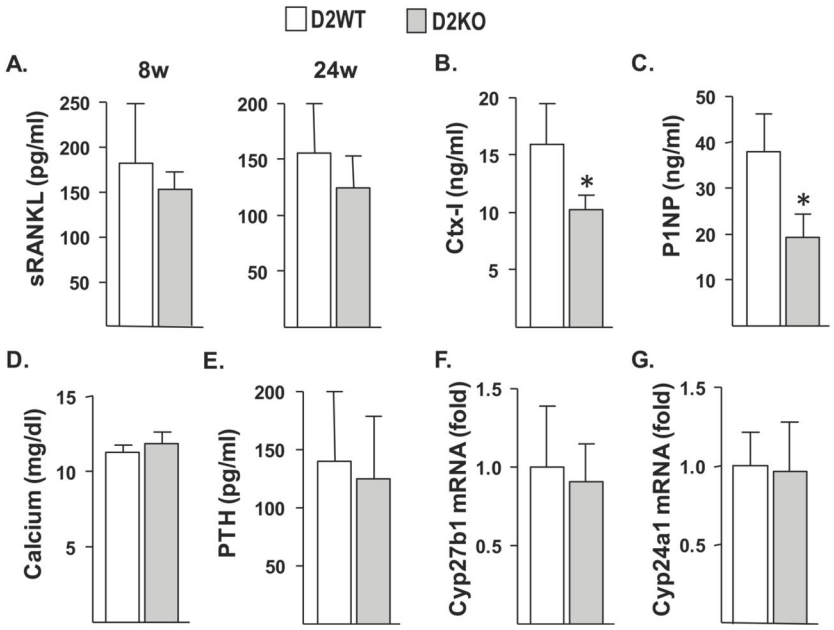

Figure 5. Lack of RL-D2 leads to decreased bone remodeling but D2KO animals maintain normal serum calcium levels

A, Circulating soluble (s) RANKL was measured in serum of 8w- and 24w-old female mice. **B–E**, Serum CTX-I (**B**), P1NP (**C**), calcium (**D**) and plasma parathyroid hormone (PTH) (**E**) levels were measured in 24w-old female mice. **F–G**, Kidney *Cyp27b1* (**F**) and *Cyp24a1* (**G**) mRNA levels of 24w-old female mice were measured by quantitative RT-PCR. All values represent mean ± SD of 5–9 animals/group. All statistical comparisons were performed using student's *t*-test. *, $p<0.05$ compared to wild type controls.

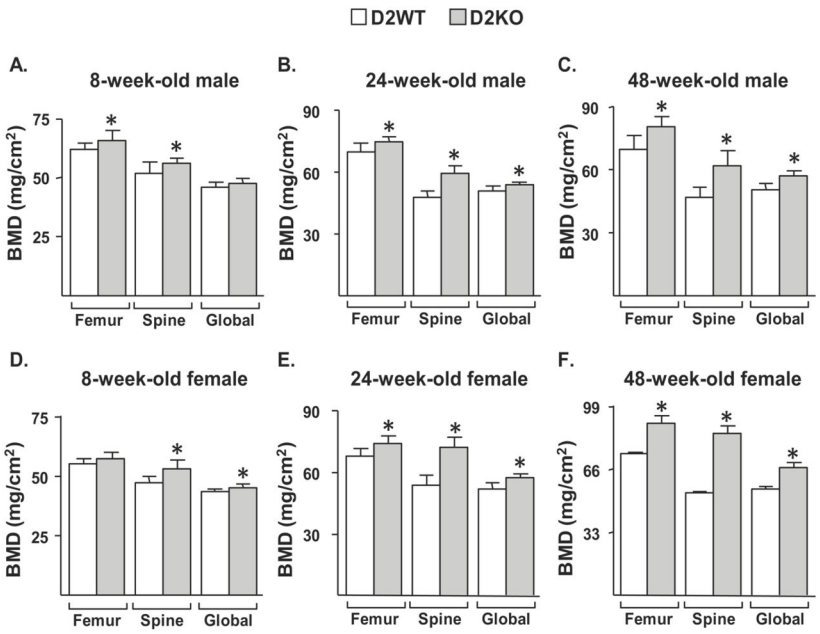

Figure 6. D2KO mice have high bone mass phenotype that becomes more pronounced with age

A–F, Femoral, vertebral and global Bone Mineral Density (BMD) of male (**A–C**) and female (**D–F**) D2KO and their wild type littermate mice was measured by PIXImus densitometer at 8w (**A,D**), 24w (**B–E**), and 48w (**C–F**) of age. **A–F**, At 8w (**A–D**) and 24w (**B–E**), all values represent mean ± SD of 5–11 animals/group, and (**C–F**) at 48w n=3–6 animals/group. All statistical comparisons within the same age group were performed using student's *t*-test. *, $p<0.05$ compared to wild type controls.

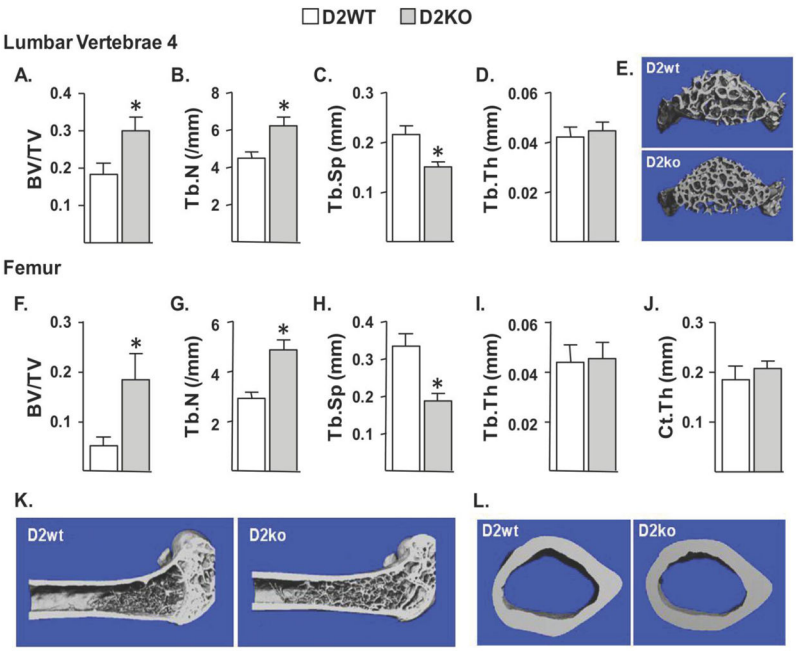

Figure 7. Lack of RL-D2 impacts cancellous, but not cortical, bone structure

µCt analysis of lumbar vertebrae 4 (L4) (**A–E**) and femurs (**F–L**) of male D2KO and their wild type littermates were performed at 12m of age. **A–J**, bone volume over tissue volume (BV/TV), trabecular number (Tb.N), trabecular separation (Tb.Sp) and trabecular thickness (Tb.Th) were measured in cancellous bones in L4 and femur. **E**, µCt image of cancellous bone in L4. **J**, cortical thickness (Ct.Th) was measured in femoral midshafts. **K–L**, µCt images of half femur (**K**) and dorsal view of the cortical bone in femoral midshaft (**L**). All statistical comparisons were accomplished using student's *t*-test. *, $p<0.05$ compared to wild type controls.

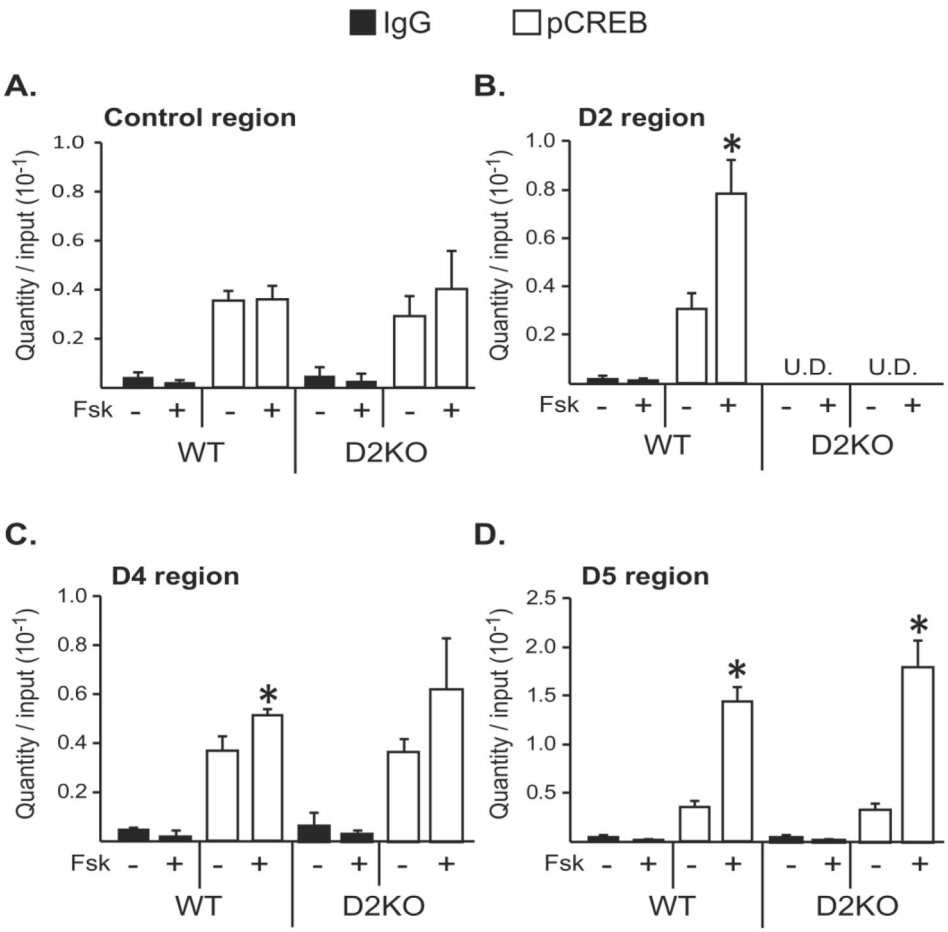

Figure 8. Lack of RL-D2 does not alter pCREB binding to RL-D4 or RL-D5

Femoral and humoral bone marrow of 9 week-old female D2WT and D2KO animals were isolated (18 mice/genotype). 10^8 cells were plated in 10 cm plates and differentiated for 9 days in osteogenic culture medium. Eighteen 10cm plates of each genotype were treated with vehicle (DMSO) or 10^6M Fsk for 1h. ChIP with IgG and pCREB was performed in triplicate, each replicate containing cells from six 10cm plates per genotype per treatment. **A–D**, pCREB binding at target sites was quantified by quantitative RT-PCR with primers targeted to −30k region of Mmp13 gene (control region) (**A**), D2 region (**B**), D4 region (**C**) and D5 region (**D**). Data are displayed as Quantity normalized to Input in triplicate ± SD. Statistical comparisons were performed using Two-Way ANOVA. *, $p<0.05$ effect of treatment within the same genotype; #, $p<0.05$ effect of genotype within the same treatment.